

Charge-state dependence of fluorine-projectile K Auger-electron production

J. Newcomb,* T. R. Dillingham, James Hall, S. L. Varghese,[†] Philip L. Pepmiller,[‡] and Patrick Richard
Department of Physics, Kansas State University, Manhattan, Kansas 66506

(Received 1 February 1984)

The K Auger-electron production cross sections of fluorine produced in collisions with thin helium- and neon-gas targets were obtained for incident fluorine ions of charge states $q=2$ to $q=8$ and incident energies of 6, 9, 12, and 15 MeV. The cross sections were measured with an electrostatic cylindrical mirror electron analyzer. The Auger transitions for the lower-charge states ($q \leq 5$) are from fluorine states created by ionization and excitation, but, for $q=6$, are from fluorine states created primarily by excitation. For the higher-charge states ($q=7$ and 8), single and double electron capture to excited states lead to the creation of autoionizing fluorine states.

I. INTRODUCTION

During the last few years, the cross sections for the three processes of K -shell ionization, K to L, M, N, \dots excitation, and electron capture for several atomic systems have been separately obtained by measuring the projectile K x rays with sufficiently high resolution to separate the different final states produced by the three processes.¹ Initial cross-section measurements²⁻⁴ were performed for the asymmetric system of $F^{q+} + \text{He}$ for $q=2-9$. More recently cross sections were measured^{5,6} for the nearly symmetric case of $F^{q+} + \text{Ne}$. These measurements provide a rather unique set of data in which the cross sections for projectile excitations have been measured as a function of the number of electrons on the projectile for a fixed nuclear charge. The ionization and excitation cross sections for the asymmetric case are understood from perturbative theories whereas those for the nearly symmetric case are not presently explained.

In order to investigate this problem in more detail, the present paper extends these measurements to the study of K Auger-electron emission from the projectile. Several problems must be dealt with when studying projectile Auger electrons. A shift of the spectra to higher energies is observed as the projectile energy increases due to the added velocity imparted to the electrons by the emitting projectiles. Also, as the projectile energy increases, or the incident charge state decreases, an exponential "background" of δ electrons becomes prominent. Finally, an increase in the observed peak width (i.e., *kinematic broadening*) occurs as the projectile energy increases.⁷

The K Auger-electron spectra for $F^{q+} + \text{He}$ and Ne at 6, 9, 12, and 15 MeV for $q=2-8$ and the corresponding K Auger-electron production cross sections have been measured in the present work. One of the interesting observations in these measurements was a very clean (i.e., almost free of background δ electrons) three-electron (Li-like) series resulting from the decay of autoionizing states. This observation was made possible by the fact that an appreciable fraction ($\sim 20\%$) of the F^{7+} was in the $1s2s(^3S)$ metastable state. Thus the F^{7+} spectra were due to autoionizing states produced by single-electron capture

to excited states of the metastable component of the beam.⁷

II. EXPERIMENTAL TECHNIQUE

The experiment was performed at the James R. Macdonald Laboratory at Kansas State University using an EN tandem Van de Graaff accelerator. The projectile K Auger-electron measurements were performed using an electrostatic cylindrical mirror analyzer to detect electrons emitted at 42° in the laboratory frame under the assumption that the emission is isotropic in the projectile's rest frame. A general discussion of the experimental techniques and procedure has been presented in detail in a previous paper in which the F^{7+} projectile K -Auger spectra and their corresponding cross sections were presented.⁷ In addition, the method of analysis as well as the particular problems inherent in the study of projectile Auger emission (e.g., Doppler shift of the spectral lines) have also been discussed in the previous paper. These items, therefore, are mentioned only in passing here.

III. DISCUSSION

The charge-state dependence of the fluorine K Auger-electron spectra for 9-MeV $F^{q+} + \text{He}$ ($q=2-8$) is shown in Figs. 1 and 2. The exponentially decreasing background observed in Fig. 1 is associated with δ electron emission. δ electrons are electrons scattered or "knocked off," mostly in the forward direction, during an ion-atom collision and, thus, the relative intensity or number of electrons so scattered is expected to vary in proportion to the number of electrons available to scatter. From Fig. 1, it can be seen that the δ electron intensity does indeed decrease as the available number of electrons in the system decreases or as q increases. Furthermore, it is seen that the intensity of the δ electron background decreases dramatically from the $q=6$ case in Fig. 1 to the $q=7$ case in Fig. 2. Granting that the number of *target* electrons available to scatter remains the same for both cases ($q=6$ and 7) and that the number of electrons available from the *projectile* differs only by one, the large decrease in the intensity of the δ electrons is due to the internal atomic structure of the projectile. The ground-state con-

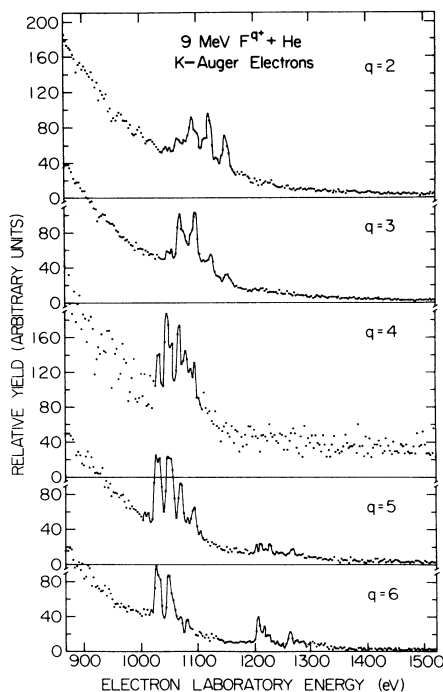


FIG. 1. The charge-state dependence of 9-MeV $F^{q+} + \text{He}$ spectra in the laboratory frame is shown for $q=2-6$.

figuration for F^{6+} is $1s^2 2s$, while the ground-state configuration for F^{7+} is $1s^2$. For both charge states, the $1s$ electrons are relatively tightly bound to the projectile, but the $2s$ electron of F^{6+} is relatively loosely bound to the

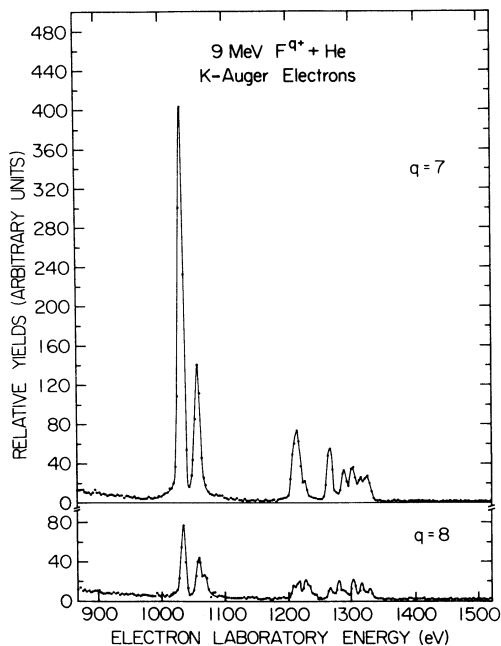


FIG. 2. The charge-state dependence of 9-MeV $F^{q+} + \text{He}$ spectra in the laboratory frame is shown for $q=7$ and 8 .

projectile and thus is expected to be “knocked off” easier than the $1s$ electrons. It can therefore be concluded from the relative intensities of the δ electrons in Figs. 1 and 2 that, for the most part, the δ electrons were originally loosely bound projectile electrons.

For a single K vacancy in an ion to decay via an Auger transition, the ion must have at least two electrons in excited states. Ion configurations having a single K vacancy and at least two electrons in an excited state can be produced, depending on the initial charge state of the ion, by electron excitation, ionization, or capture processes. For the case of F^{7+} (cf. Fig. 2), these configurations and the resulting spectrum can be produced if the fluorine projectile undergoes single electron capture of a target electron into an excited state of the metastable projectile. The F^{7+} spectra was discussed in more detail in previous papers.^{7,8} These same configurations, resulting in the corresponding spectrum in Fig. 2, can be produced with a F^{8+} projectile if the projectile undergoes double electron capture from the target into excited states of the projectile.

Since the projectile ions illustrated in Fig. 1 have no initial K vacancy, simple capture of an electron into an excited state will not result in a K -Auger transition. Therefore, for charge states of $q=2$ through $q=6$, either excitation or ionization of a K -shell electron is necessary to produce a K -Auger spectrum. A comparison between Figs. 1 and 2 shows that the F^{6+} spectrum, without the large δ electron background, strongly resembles the F^{7+} and F^{8+} spectra in Fig. 2 and should arise from the same configurations. The necessary configurations are produced in F^{6+} by excitation of a single K -shell electron. Note that single K -shell ionization will not lead to autoionizing states for this charge state.

Excitation of a single K -shell electron can produce a K -Auger transition for the remaining charge states of fluorine as well (i.e., $q < 6$), but the competing process, ionization of a single K -shell electron, also produces configurations for these charge states which can result in a K -Auger transition. In particular, if F^{5+} undergoes ionization of a single K -shell electron, the same configurations resulting in the spectra of Fig. 2 can be produced and peaks corresponding in electron energy to the peaks in Fig. 2 are seen. The charge-state dependence of the cross sections for single K -shell electron ionization and single K -shell electron excitation in fluorine has been previously studied by Tawara *et al.*² It was shown that the ratio of the K -shell excitation process to the K -shell ionization process decreases as the incident projectile charge state decreases. Thus K -shell ionization is more important for the lower charge states while K -shell excitation is more important for the higher charge states.

The charge state dependence of the projectile K -Auger production cross sections is shown in Fig. 3 for the cases of 9-MeV $F^{q+} + \text{He}$ and 9-MeV $F^{q+} + \text{Ne}$ and are representative of the charge-state dependences at other projectile energies. The lines are to guide the eye, with the horizontal lines being, in each case, the weighted average of the cross sections for the charge states $q=2$ through $q=6$. The cross sections for the charge states $q=2$ through $q=5$ are the sum of the K -shell ionization cross

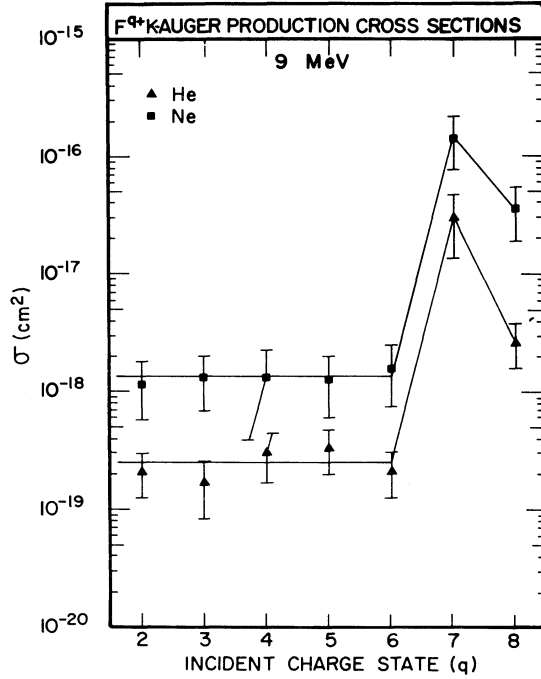


FIG. 3. The incident charge-state dependence of 9-MeV F^{q+} K -Auger production cross sections is shown for helium and neon gas targets. The lines are drawn to guide the eye.

section, which is decreasing with increasing charge state, and the K -shell excitation cross section, which is increasing with increasing charge state. The trend of the charge-state dependence shown in Fig. 3 bears a strong resemblance to the charge-state dependences of previously

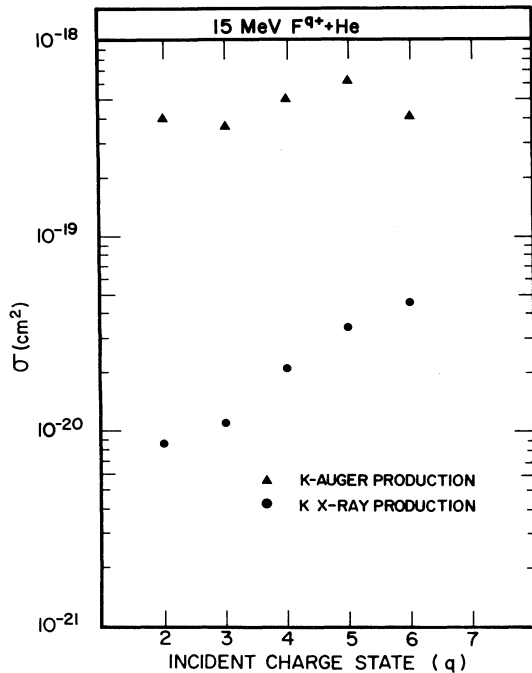


FIG. 4. The incident charge-state dependences for the K -Auger production and the K x-ray production cross sections are shown for 15-MeV $F^{q+} + \text{He}$.

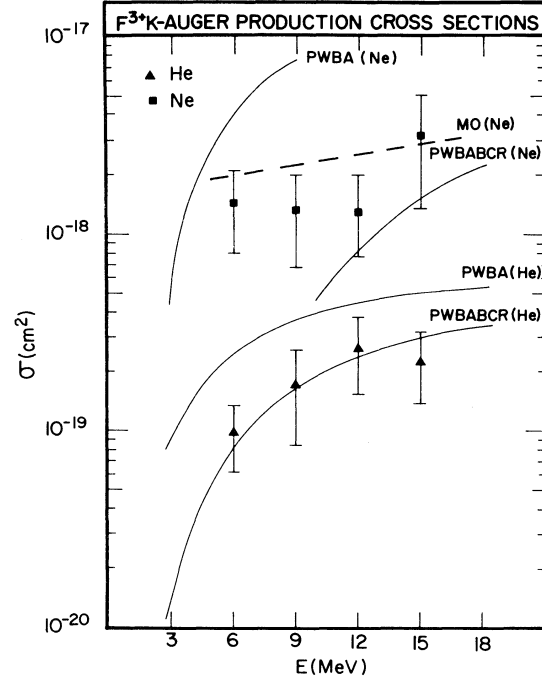


FIG. 5. The energy dependence of F^{3+} K -Auger production cross sections for helium and neon gas targets are compared to a PWBA calculation and a PWBA calculation including binding, Coulomb deflection, and relativistic effects (PWBABCRC). The dashed line is the molecular orbital (MO) prediction using the rotational-coupling model of Taulbjerg *et al.* (Ref 18).

measured K x-ray cross sections.⁹⁻¹¹ The major difference is the K -Auger production cross section for the incident one-electron ion which is much smaller than that for the two-electron ion. For the x-ray case, single capture into an excited state of a one-electron ion can result in a K x-ray transition but not in a K -Auger transition. Double capture to an excited state, a process with a much lower probability than single capture,¹² can result in a K -Auger transition.

A comparison between the K -Auger and K x-ray production cross sections for 15-MeV $F^{q+} + \text{He}$ ($q=2-6$) is presented in Fig. 4. Since the error in the 15-MeV F^{q+} data is larger than the errors in the data for the other projectile energies in this study, the K -Auger production cross sections are extrapolated from the energy dependences of the various fluorine incident charge states. The

TABLE I. Average fluorescence yields ($\times 100$) for various incident charge states, q , of F^{q+} ions corresponding to some average emitting charge state.

q	$\bar{\omega}_{\text{expt}}(q)$	$\bar{\omega}_{\text{th}}(q)^a$	$\bar{\omega}_{\text{expt}}(q)/\bar{\omega}_{\text{th}}(q)$
2	2.09	2.69	0.78
3	3.09	3.86	0.80
4	3.99	6.65	0.60
5	5.12	11.0	0.47
6	13.5	18.6	0.73

^aCalculated from values of $\bar{\omega}_{\text{th}}(q_{\text{em}})$ for a specific emitting charge state, q_{em} , found in Ref. 2.

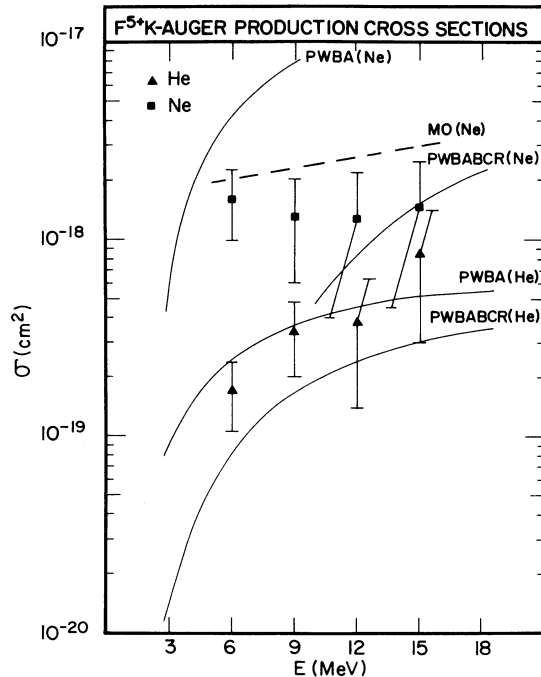


FIG. 6. The energy dependence of F^{5+} K -Auger production cross sections for helium and neon gas targets are compared to a PWBA calculation and a PWBA calculation including binding, Coulomb deflection, and relativistic effects (PWBABC). The dashed line is the molecular orbital (MO) prediction using the rotational-coupling model of Taulbjerg *et al.* (Ref. 18).

K x-ray production cross sections are from Tawara *et al.*² and correspond to the x-ray decay of those configurations of fluorine which can also produce a K -Auger electron. From the cross sections of Fig. 4, the average fluorescence yield can be calculated for each incident charge state using the equation

$$\bar{\omega}_{\text{expt}}(q) = \frac{\sigma_x(q)}{\sigma_x(q) + \sigma_A(q)},$$

where $\sigma_x(q)$ is the K x-ray production cross section and $\sigma_A(q)$ is the corresponding K -Auger production cross section for a given incident charge state q . The values of $\bar{\omega}_{\text{expt}}(q)$ are tabulated in Table I for each incident charge state along with the estimated theoretical fluorescence yields, $\bar{\omega}_{\text{th}}(q)$ and the ratio $\bar{\omega}_{\text{expt}}(q)/\bar{\omega}_{\text{th}}(q)$. The predicted fluorescence yields, $\bar{\omega}_{\text{th}}(q)$, were estimated from the values for the configuration averaged fluorescence yield for a

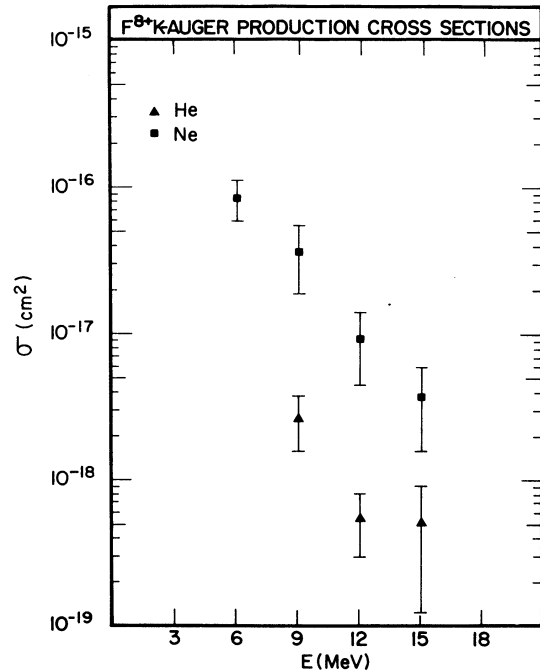


FIG. 7. The energy dependence of F^{8+} K -Auger production cross sections for helium and neon gas targets are shown. The cross sections are a measure of double electron capture to excited states of fluorine.

specific emitting charge state, $\bar{\omega}_{\text{th}}(q_{\text{em}})$,² and are defined by the relation

$$\bar{\omega}_{\text{th}}(q) = \frac{\sum \sigma_x(q_{\text{em}})}{\sum [\sigma_x(q_{\text{em}})/\bar{\omega}_{\text{th}}(q_{\text{em}})]},$$

where $\sigma_x(q_{\text{em}})$ represents the K x-ray production cross section² for a given emitting charge state, q_{em} . As can be seen in Table I, $\bar{\omega}_{\text{expt}}(q)$ is consistently smaller than $\bar{\omega}_{\text{th}}(q)$ by as much as $\sim 50\%$ for $q = 5$ and as little as $\sim 20\%$ for $q = 3$. The differences may be due to a systematic error artificially raising the K -Auger production cross sections or lowering the K x-ray production cross sections, thus making $\bar{\omega}_{\text{expt}}(q)$ too small. On the other hand, the configuration averaged fluorescence yields $\bar{\omega}_{\text{th}}(q_{\text{em}})$ used to calculate $\bar{\omega}_{\text{th}}(q)$ may be too large. Overall, the agreement between $\bar{\omega}_{\text{expt}}(q)$ and $\bar{\omega}_{\text{th}}(q)$ is reasonable.

The energy dependences of the K -Auger production cross sections for F^{3+} and F^{5+} projectiles incident upon both target gases (i.e., He and Ne) are presented in Figs. 5

TABLE II. Fluorine K -Auger production cross sections in units of 10^{-19} cm^2 for $F^{q+} + \text{He}$.

q	3 MeV	6 MeV	9 MeV	12 MeV	15 MeV
2	0.53 ± 0.19	2.35 ± 0.51	2.11 ± 0.86	3.82 ± 1.65	
3		0.97 ± 0.36	1.70 ± 0.86	2.62 ± 1.10	2.27 ± 0.90
4		1.33 ± 0.57	3.02 ± 1.31	2.69 ± 1.16	4.96 ± 2.26
5		1.70 ± 0.66	3.35 ± 1.37	3.77 ± 2.40	8.39 ± 5.42
6		0.89 ± 0.25	2.14 ± 0.88	2.09 ± 1.01	4.22 ± 4.26
7		1670 ± 825	303 ± 166	77.0 ± 42.3	34.2 ± 19.2
8			26.5 ± 10.7	5.51 ± 2.53	5.17 ± 3.94

TABLE III. Fluorine *K*-Auger production cross sections in units of 10^{-18} cm² for $F^{q+} + \text{Ne}$.

q	6 MeV	9 MeV	12 MeV	15 MeV
2	1.38±0.41	1.18±0.60		
3	1.44±0.65	1.33±0.65	1.31±0.54	3.19±1.84
4	1.73±0.69	1.31±0.93	0.98±0.56	1.34±0.80
5	1.60±0.62	1.29±0.69	1.28±0.87	1.44±0.99
6	1.55±0.61	1.59±0.84	8.69±5.45	1.69±0.82
7	434±170	147±69.1	46.2±24.3	20.5±10.8
8	84.8±25.9	36.7±17.7	9.38±4.88	3.79±2.17

and 6, respectively, and are representative of the energy dependences for the charge states ($q=2-6$). Also plotted for comparison are two plane-wave Born calculations for each system: a plane-wave Born approximation¹³ (PWBA) and a PWBA calculation with binding, Coulomb deflection, and relativistic corrections added (PWBA+BCR).^{14,15} In both figures, the helium data, within the errors, fall between the two calculations. It should be remembered that the two calculations are for *K*-shell ionization, whereas, the experimental cross sections for both charge states contain some contribution from *K*-shell excitation. If excitation were included, the calculations would predict larger cross sections than depicted in Figs. 5 and 6. The increase would be larger in the F^{5+} case than in the F^{3+} case.²

The *K*-Auger production cross sections for F^{3+} and F^{5+} on neon display a flatter energy dependence over the observed energy range than the helium data, whereas, the PWBA calculations indicate that the energy dependence should be much steeper. The *K* excitation of the nearly symmetric system of fluorine on neon is not expected to follow a perturbative theory, but rather should follow a molecular excitation theory. Neon *K*-shell excitation in the fluorine on neon case has been studied by Woods *et al.*¹⁶ and Hagmann *et al.*¹⁷ The total cross section, as well as the impact parameter dependence, is in good agreement with the rotational-coupling model prediction of Taulbjerg *et al.*¹⁸ with an occupation number, n_π of ~ 0.35 for the $2p\pi_x$ molecular orbital. The relative *K*-vacancy production cross sections for fluorine and neon can be deduced from the *K*-vacancy sharing model of Meyerhof.¹⁹ The resulting predicted cross section is in excellent agreement with the present data over the energy range of 6–15 MeV as shown in Figs. 5 and 6. The predicted molecular orbital cross section drops rather abruptly below 2 MeV bombarding energy.

Figure 7 presents the energy dependences of the *K*-Auger production cross sections for F^{8+} on both helium and neon. The *K*-Auger production cross sections in Fig. 7 are for double electron capture forming doubly excited states of F^{6+} . These energy dependences follow those of single electron capture very well^{5,9} and match the double electron capture results obtained by a final charge-state analysis.¹² For completeness, the fluorine *K*-Auger pro-

duction cross sections, including errors, are presented in Table II for helium and in Table III for neon. The helium data are in units of 10^{-19} cm², while the neon data are in units of 10^{-18} cm².

IV. CONCLUSION

The fluorine projectile *K* Auger-electron production cross sections in ion-atom collisions have been measured for a variety of incident charge states and incident energies and for two target gases. These data extend the previous work of Woods *et al.*¹⁶ to higher charge states. The incident charge state dependence of the projectile *K* Auger cross sections was found to closely resemble the charge-state dependence of corresponding x-ray measurements.⁹⁻¹¹ The only major difference was for the incident one-electron ion ($q=8$) where double capture is necessary to produce a *K*-Auger satellite while, in the x-ray case, single capture is sufficient to produce a *K* x-ray satellite. For $q \leq 6$, the differences between the Auger measurements and the x-ray measurements were assumed to be due to the incident charge-state dependence of the average fluorescence yields. The average fluorescence yield as a function of incident projectile charge state was determined by combining the Auger and x-ray measurements² for 15-MeV fluorine and compare reasonably well with theoretical calculations.

The energy dependences of the projectile *K*-Auger production cross sections were almost identical for fluorine charge states of $q=2-6$. Furthermore, for the helium target, the energy dependence of the *K*-Auger production cross sections agreed well with a simple PWBA calculation¹³ and a PWBA calculation with binding, Coulomb deflection, and relativistic corrections included.^{14,15} For the nearly symmetric case of fluorine on neon, the magnitude and energy dependence of the cross sections agree quite well with the rotational-coupling model of Taulbjerg *et al.*¹⁸

ACKNOWLEDGMENT

This work was supported by the U. S. Department of Energy (Division of Chemical Sciences).

- *Present address: National Space Technology Laboratories, Naval Ocean Research and Development Activity, U.S. Department of the Navy, code 245, NSTL Station, MS 39529.
- †Permanent address: University of South Alabama, Mobile, AL 36688.
- ‡Present address: Oak Ridge National Laboratory, Oak Ridge, TN 37830.
- ¹F. Hopkins, R. L. Kauffman, C. W. Woods, and P. Richard, *Phys. Rev. A* **9**, 2413 (1974).
- ²H. Tawara, P. Richard, K. A. Jamison, T. J. Gray, J. Newcomb, and C. Schmiedekamp, *Phys. Rev. A* **19**, 1960 (1979).
- ³H. Tawara, P. Richard, K. A. Jamison, and T. J. Gray, *J. Phys. B* **11**, L619 (1978).
- ⁴H. Tawara, M. Terasawa, P. Richard, T. J. Gray, P. Pepmiller, J. Hall, and J. Newcomb, *Phys. Rev. A* **20**, 2340 (1979).
- ⁵P. Richard, P. L. Pepmiller, and K. Kawatsura, *Phys. Rev. A* **25**, 1937 (1982).
- ⁶P. L. Pepmiller and P. Richard, *Phys. Rev. A* **26**, 786 (1982).
- ⁷J. Newcomb, T. R. Dillingham, J. Hall, S. L. Varghese, P. L. Pepmiller, and P. Richard, *Phys. Rev. A* **29**, 82 (1984).
- ⁸T. R. Dillingham, J. Newcomb, J. Hall, P. Pepmiller, and P. Richard, *Phys. Rev. A* **29**, 3029 (1984).
- ⁹M. Terasawa, T. J. Gray, S. Hagmann, J. Hall, J. Newcomb, P. Pepmiller, and P. Richard, *Phys. Rev. A* **27**, 2868 (1983).
- ¹⁰M. D. Brown, L. D. Ellsworth, J. A. Guffey, T. Chiao, E. W. Pettus, L. M. Winters, and J. R. Macdonald, *Phys. Rev. A* **10**, 1255 (1974).
- ¹¹J. R. Macdonald, M. D. Brown, S. J. Czuchlewski, L. M. Winters, R. Laubert, I. A. Sellin, and J. R. Mowat, *Phys. Rev. A* **14**, 1997 (1976).
- ¹²S. M. Ferguson, J. R. Macdonald, T. Chiao, L. D. Ellsworth, and S. A. Savoy, *Phys. Rev. A* **8**, 2417 (1973).
- ¹³G. S. Khandalwal, B. H. Choi, and E. Merzbacher, *At. Data* **1**, 103 (1969).
- ¹⁴G. Basbas, W. Brandt, and R. Laubert, *Phys. Rev. A* **7**, 983 (1973).
- ¹⁵G. Basbas, W. Brandt, and R. Laubert, *Phys. Rev. A* **17**, 1655 (1978).
- ¹⁶C. W. Woods, R. L. Kauffman, K. A. Jamison, N. Stolterfoht, and P. Richard, *Phys. Rev. A* **13**, 1358 (1976).
- ¹⁷S. Hagmann, C. L. Cocke, J. R. Macdonald, P. Richard, H. Schmidt-Böcking, and R. Schuch, *Phys. Rev. A* **25**, 1918 (1982).
- ¹⁸K. Taulbjerg, J. Briggs, and J. Vaaben, *J. Phys. B* **9**, 1351 (1976).
- ¹⁹W. E. Meyerhof, *Phys. Rev. Lett.* **31**, 1341 (1973).